THE ASTRONOMICAL JOURNAL VOLUME 84, NUMBER 11 NOVEMBER 1979

THE PHOTOMETRIC BEHAVIOR OF Be STARS

A. FEINSTEIN [a),b)] and H. G. MARRACO [b)]

Observatorio Astronómico, Universidad Nacional de La Plata, 1900 La Plata, Argentina

Received 18 May 1979

ABSTRACT

We present photometric data for 76 Be stars observed in ***UBV*** and in the Balmer lines Hα, Hβ, and Hγ. An ultraviolet excess, derived from the Q value, appears as a common feature for nearly all them. From a statistical study of the data, the percentages of variability are: 77% in V, 48% in $B-V$, and 68% in $U-B$. The amounts of emission in the α and β indices, which we call e_α and e_β, are computed. It is demonstrated that both emission indices are very well correlated to the spectroscopic emission features, their equivalent widths, and possibly also to the ultraviolet excess. The correlation of the standard deviation of the V magnitude with the projected rotational velocity is in agreement with a model in which the Balmer line emission is due to a gaseous ring. The observed β values corrected for the emission indices become good indicators of the absolute magnitudes, as is confirmed by a sample of Be stars known to be members of clusters and associations. Some properties of the galactic distribution of the Be stars are then derived from our results.

I. INTRODUCTION

The study of Be stars permits us to obtain information on early-type stars with gaseous envelopes. Photometric changes and rapid variations of the structure of the emission lines indicate instabilities in their envelopes. Nevertheless, not all of them display the same activity.

As was pointed out by Feinstein (1968), and Ferrer and Jaschek (1971) about 50% of the Be stars show some kind of photometric variations. A survey of Hydrogen line indices from narrow band photometry revealed also changes of the Hβ line intensities (Feinstein 1973).

On the other hand, the separation of the Be-type stars from the supergiants using photometric methods was investigated several times with positive results (Abt and Golson 1966; Crawford, Barnes, and Perry 1975).

The present work tries to throw some light on the activity of the envelopes of bright Be stars with measures derived from the commonly used *UBV* system and from the Hydrogen Balmer lines. This gives us the possibility to compare them with normal stars, even though the *UBV* system is not the most appropriate one for these particular stars.

With this aim in mind, we present here an extended series of observations of about 76 stars in the *UBV* system covering over 15 years and narrow band Hydrogen line measures spanning over eight years.

The 76 selected stars are mostly those found to have Hydrogen line emission by Jaschek, Jaschek, and Kucewicz (1964) in a systematic survey of B-type stars covering the years 1960–1962.

Section 2 includes the final results of the observations obtained in the *UBV*. Section 3 refers to the data on the Balmer lines. The definition of the emission indices is presented in Sec. 4, and in Sec. 5 their relation to the rotational velocities is indicated. Section 6 gives the galactic distribution properties, and finally a conclusion with regard to all the preceding information is presented in Sec. 7.

II. THE *UBV* DATA

The mean values of V, $B-V$, and $U-B$ from all the measures between 1963 and 1976 are listed in Table I, which also includes the HD and HR designations, the number of measures, the dispersions in magnitude and in each color, and the spectral types taken mostly from Lesh (1968), and Hiltner, Garrison, and Schild (1969). The references to the sources of the spectral types are listed at the bottom of Table I. The data already published (Feinstein 1968, 1975) are also included in this table.

The errors of the listed values depend strongly on the place where the measures were obtained. They are smaller at Cerro Tololo $\epsilon_{CT} = \pm 0.015$ than at La Plata $\epsilon_{LP} = \pm 0.020$ (per single observations).

The two color ($U-B$, $B-V$) array for all the observed Be stars is presented in Fig. 1. The main sequence relation (FitzGerald 1970) appears as a left envelope for all of them. It is evident that the observed Be stars are affected by reddening to some extent, but it is obvious that in many of them another effect due to the ultraviolet excess is also present. This is clearly shown by Figs. 2 and

[a)] Visiting Astronomer, Cerro Tololo Inter-American Observatory, which is operated by the Association of Universities for Research in Astronomy, Inc., under contract with the National Science Foundation, USA.

[b)] Member of the Carrera del Investigador Científico, Consejo Nacional de Investigaciones Científicas y Técnicas, Argentina.

TABLE I. UBV data for the Be stars.

HD	HR	V	$B-V$	$U-B$	n	σ_V	σ_{B-V}	σ_{U-B}	Sp. T.	Refs
28497	1423	5.44	−0.14	−0.97	27	0.035	0.017	0.035	B1.5 Ve_2	a
30076	1508	5.85	−0.08	−0.80	28	0.074	0.027	0.034	B2 Ve_2	a
35165	1772	6.08	−0.19	−0.68	24	0.022	0.009	0.032	B5 IVnp	b
37795	1956	2.66	−0.12	−0.39	24	0.012	0.008	0.032	B8 Ve	c
41335	2142	5.22	−0.08	−0.85	22	0.016	0.015	0.034	B2 $Ve_3 + n$	a
42054	2170	5.84	−0.14	−0.56	27	0.028	0.018	0.036	B4 IVe_1+	b
43544	2249	5.93	−0.16	−0.78	28	0.038	0.026	0.043	B2.5 Ve_1n	a
44458	2284	5.55	0.01	−0.84	29	0.041	0.014	0.033	B1 Ve_2+	a
45677	FS CMa	8.24	0.04	−0.68	19	0.161	0.017	0.030	B2 IVe	d
45910	AX Mon	6.80	0.34	−0.60	22	0.039	0.027	0.084	B0.5 + K2II	e
48917	2492	5.34	−0.15	−0.88	25	0.086	0.031	0.057	B2 IIIe	b
50013	2538	3.87	−0.20	−0.97	22	0.091	0.036	0.045	B1.5 $IVne_2$	b
52437	2628	6.53	−0.18	−0.81	18	0.060	0.018	0.061	B2 IV-V	b
54309	2690	5.85	−0.14	−0.87	22	0.055	0.022	0.037	B2 IVe	b
56014	2745	4.65	−0.17	−0.74	43	0.084	0.017	0.105	B3 IIIp	b
56139	2749	3.86	−0.14	−0.73	25	0.102	0.031	0.042	B2 IV-Ve_1+	b
57150	2787	4.65	−0.10	−0.80	18	0.049	0.011	0.036	B2 $IVne_2$	b
58155	2819	5.42	−0.17	−0.67	19	0.019	0.016	0.024	B4 Vnp	b
58343	2825	5.37	−0.07	−0.58	16	0.054	0.031	0.034	B2.5 IVe_1	a
58978	2855	5.60	−0.11	−1.01	16	0.052	0.013	0.037	B0.5 IVnpe	b
60606	2911	5.45	−0.09	−0.73	23	0.059	0.022	0.034	B3 Vne_2	b
60855	2921	5.71	−0.12	−0.70	5	0.007	0.006	0.014	B2 Ve_1	a
61925	2968	6.02	−0.05	−0.42	17	0.025	0.016	0.035	B6 IV	b
63462	3034	4.48	−0.09	−1.02	18	0.014	0.052	0.028	B1 IV?nne_2	b
65875	3135	6.50	−0.10	−0.78	15	0.035	0.024	0.036	B2.5 Ve_3+	a
66194	3147	5.82	−0.08	−0.76	11	0.034	0.007	0.029	B2 IVpne	b
67888	3195	6.34	−0.05	−0.54	18	0.064	0.040	0.025	B4 Ve	b
68980	3237	4.73	−0.12	−0.97	18	0.106	0.026	0.029	B1.5 IIIe	b
72067	3356	5.84	−0.17	−0.72	16	0.049	0.008	0.035	B2 V	b
75311	3498	4.48	−0.17	−0.76	14	0.043	0.014	0.064	B3 Vne	b
77320	3593	6.08	−0.17	−0.79	18	0.027	0.030	0.020	B3 Vne_1	b
78764	3642	4.70	−0.16	−0.82	17	0.064	0.022	0.020	B2 IVe_1	b
83953	3858	4.77	−0.11	−0.57	20	0.025	0.015	0.018	B6 Ve_1+	b
86612	3946	6.21	−0.10	−0.66	19	0.076	0.025	0.042	B4 Ve_2+	b
88661	4009	5.70	−0.08	−0.91	26	0.066	0.015	0.018	B2 IVpne	b
88825	4018	6.11	−0.08	−0.49	16	0.026	0.011	0.013	B4 Ve	b
89890	4074	4.48	−0.01	−0.55	2				B3 III	b
91465	4140	3.30	−0.11	−0.71	14	0.037	0.016	0.018	B4 Vne_2	b
92964	4198	5.38	0.25	−0.66	15	0.019	0.018	0.017	B2.5 Ia	b
102776	4537	4.35	−0.16	−0.61	17	0.027	0.019	0.033	B3 V	b
105435	4621	2.57	−0.13	−0.92	10	0.016	0.004	0.024	B2 $IVne_2$+	b
105521	4625	5.58	−0.08	−0.63	6	0.033	0.014	0.017	B3 IV	b
106911	4674	4.24	−0.13	−0.52	13	0.015	0.005	0.023	B5 Vn	b
110432	4830	5.34	0.22	−0.84	18	0.031	0.031	0.023	B2?pe	b
112078	4897	4.63	−0.16	−0.62	17	0.012	0.014	0.018	B4 Vn	b
112091	4899	5.07	−0.08	−0.60	15	0.059	0.021	0.015	B5 Vne_1+	b
113120	4930	5.99	0.02	−0.90	15	0.040	0.023	0.038	B1.5 $IIIne_2$+	b
115842	5027	6.03	0.29	−0.71	18	0.022	0.017	0.031	B0.5 Ia	b
120307	5190	3.42	−0.22	−0.89	19	0.016	0.013	0.017	B2 IV	b
120324	5193	3.34	−0.17	−0.91	17	0.133	0.027	0.064	B2 IV-Ve	b
120991	5223	6.06	−0.07	−0.92	19	0.123	0.041	0.036	B2 IIIe	b
124367	5316	5.03	−0.06	−0.63	18	0.032	0.015	0.015	B4 Vne_2	b
127972	5440	2.38	−0.22	−0.85	16	0.035	0.015	0.031	B1.5 Vn	b
131492	5551	5.18	0.03	−0.75	19	0.129	0.015	0.074	B4 Vnp	b
137387	5730	5.50	−0.12	−0.77	17	0.051	0.021	0.051	B1 pne	b
142983	5941	4.87	−0.08	−0.22	21	0.070	0.029	0.180	B5 IIIp	a
148184	6118	4.55	0.22	−0.79	18	0.079	0.024	0.059	B1.5 Ve_4	a
148379	6131	5.34	0.54	−0.46	16	0.025	0.029	0.032	B1.5 Iap	b
148688	6142	5.32	0.34	−0.65	15	0.030	0.024	0.034	B1 Ia+	b
149404	6164	5.46	0.39	−0.65	15	0.020	0.018	0.037	O9 Ia	b
152235	6261	6.34	0.51	−0.47	12	0.031	0.032	0.031	B1 Ia	b
152236	6262	4.73	0.48	−0.55	12	0.025	0.014	0.033	B1.5 Ia + p	b
152667	6283	6.38	0.19	−0.73	4				B0.5 Ia	b
154090	6334	4.86	0.25	−0.70	8	0.020	0.021	0.037	B1 Ia	b
155806	6397	5.52	0.01	−0.97	6	0.026	0.017	0.042	O8 Ve_2	b
157042	6451	5.22	−0.11	−0.84	7	0.028	0.022	0.030	B2 $IIIne_2$	b
158427	6510	2.93	−0.16	−0.72	6	0.057	0.018	0.030	B2 Vne_2	b
167128	6819	5.36	−0.06	−0.67	13	0.027	0.012	0.040	B3 IIIpe	b
173948	7074	4.21	−0.15	−0.88	15	0.038	0.016	0.029	B2 II–III	b
178175	7249	5.51	−0.06	−0.67	17	0.086	0.011	0.027	B2 Ve_1	a
205637	8260	4.62	−0.19	−0.64	16	0.051	0.011	0.042	B2.5 Vp	a
209014	8386	5.43	−0.10	−0.30	16	0.048	0.011	0.023	B8 V	c
209409	8402	4.71	−0.11	−0.39	13	0.016	0.013	0.033	B7 IVe_1	a
209522	8408	5.95	−0.17	−0.65	13	0.029	0.011	0.027	B5 Vn	c

TABLE I. (Continued).

HD	HR	V	$B-V$	$U-B$	n	σ_V	σ_{B-V}	σ_{U-B}	Sp. T.	Refs
212571	8539	4.49	0.02	−1.01	4				B1 Ve_1	a
214748	8628	4.17	−0.11	−0.31	18	0.037	0.013	0.029	B8 Ve	c

[a] Lesh (1968).
[b] Hiltner *et al.* (1969).
[c] Bright Star Catalogue.
[d] Burnichon *et al.* (1967).
[e] Polidan and Peters (1976).

3, where we plotted the spectral type versus the $B-V$ color in the former, and versus the $U-B$ color in the latter. In the first case, all the stars are below the standard sequence of FitzGerald, but in the second one the stars appear scattered around it. The clearest explanation for this particular distribution is the already mentioned ultraviolet excess affecting mainly the $U-B$ color. The supergiant stars are not included in either diagram.

As the ultraviolet excess is independent of reddening, we can use this fact to measure its amount. This may be done through the reddening-free Q value which is defined by $Q_{\rm UBV} = U-B-(E_{U-B}/E_{B-V})(B-V)$. We can also get another value of Q from the spectral classification ($Q_{\rm ST}$), and the calibration of Gutierrez-Moreno (1975). Both Q's are given in Table II. The difference $Q_{\rm ST} - Q_{\rm UBV} = \Delta Q$ gives for each star a value which is related to the ultraviolet emission. This difference ΔQ is mostly negative as many of the Be stars have a smaller Q value (more negative) than the one which they would have if no ultraviolet excess was present.

Let us now consider the photometric variability. The 73 Be stars of Table I with five or more observations were compared to 10 B-type stars purposely observed at the same nights along with the Be stars' program.

In order to obtain the percentage of Be stars that are variable, we proceeded as follows: (1) The dispersion distribution of the Be stars in each color and in the V magnitude was thought of as being the sum of two distributions: that of the nonvariable and that of the variable Be stars. (2) The shape of the nonvariable Be stars distributions was adopted from the comparison B-type stars. (3) The contribution of the variable star distri-

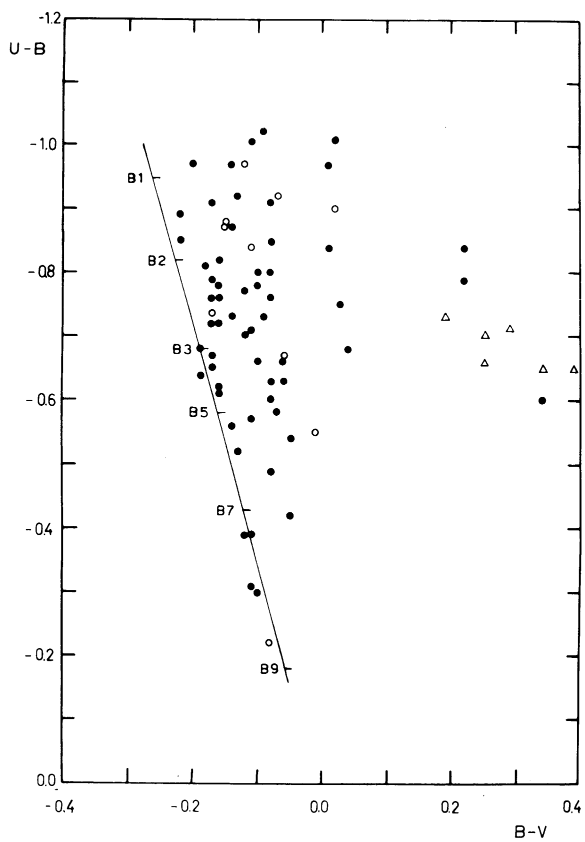

FIG. 1. The $(U-B, B-V)$ diagram of the observed Be stars. The full circles correspond to dwarf stars, the open circles to giants, and the triangles to supergiants. The solid line represents the main sequence taken from FitzGerald (1970).

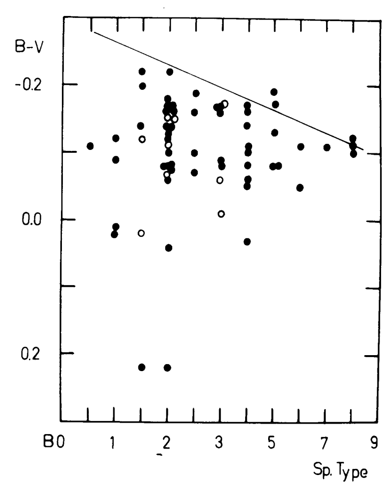

FIG. 2. The observed $B-V$ color vs the spectral type for the Be stars. FitzGerald's main sequence is indicated by a solid line. The symbols for the stars are the same as in Fig. 1.

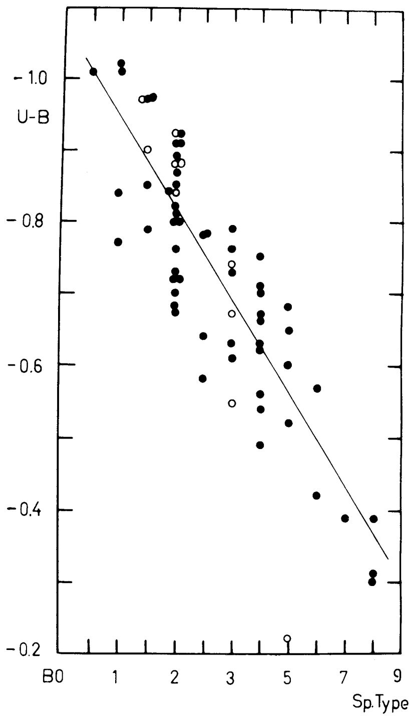

FIG. 3. The observed $U - B$ color vs the spectral type. The symbols are the same as in Fig. 2.

bution was considered negligible between zero and a certain limit. (4) These limits were chosen as close as possible to the maximum of the non-variable stars distribution. Their values are $0^m_.025$, $0^m_.015$, and $0^m_.020$ in the V, $B - V$, and $U - B$, respectively. (5) The dispersion distributions for the Be and the comparison B-type stars were matched between zero and the quoted limits using the χ^2 criterion. (6) The percentage of variable Be stars was obtained by subtracting both distributions appropriately scaled.

Table III shows the percentage of variability derived from every magnitude and color. As a comparison, the results obtained by Ferrer and Jaschek (1971) are also included. The limits used in both investigations not only have different values but also different meanings as explained in the notes to the Table.

Our data are presented in Fig. 4, where the dark area is the inferred distribution of the fraction considered nonvariable. The χ^2 distribution was used to represent the shape of the dark area for values larger than the limits quoted above.

TABLE II. Determination of the ultraviolet excesses through the Q values.

HD	Q_{UBV}	Q_{ST}	ΔQ
28497	−0.875	−0.754	−0.121
30076	−0.746	−0.722	−0.024
35165	−0.561	−0.456	−0.105
41335	−0.796	−0.722	−0.074
42054	−0.471	−0.522	0.051
43544	−0.675	−0.656	−0.019
44458	−0.847	−0.785	−0.062
48917	−0.780	−0.722	−0.058
50013	−0.834	−0.754	−0.080
52437	−0.689	−0.722	0.033
54309	−0.776	−0.722	−0.054
56014	−0.630	−0.589	−0.041
56139	−0.636	−0.722	0.086
57150	−0.733	−0.722	−0.011
58155	−0.562	−0.522	−0.040
58343	−0.534	−0.656	0.122
58978	−0.933	−0.830	−0.103
60606	−0.672	−0.589	−0.083
60855	−0.620	−0.722	0.102
61925	−0.389	−0.393	0.004
63462	−0.958	−0.785	−0.173
65875	−0.715	−0.656	−0.059
66194	−0.706	−0.722	0.016
67888	−0.508	−0.522	0.014
68980	−0.889	−0.754	−0.135
72067	−0.606	−0.722	0.116
75311	−0.650	−0.589	−0.061
77320	−0.680	−0.589	−0.091
78764	−0.713	−0.722	0.009
83953	−0.502	−0.393	−0.109
86612	−0.597	−0.522	−0.075
88661	−0.856	−0.722	−0.134
88825	−0.439	−0.522	0.083
89890	−0.544	−0.589	0.045
91465	−0.640	−0.522	−0.118
102776	−0.507	−0.589	0.082
105435	−0.833	−0.722	−0.111
105521	−0.578	−0.589	0.011
106911	−0.439	−0.456	0.017
110432	−0.987	−0.722	−0.265
112078	−0.518	−0.522	0.004
112091	−0.550	−0.454	−0.096
113120	−0.914	−0.754	−0.160
120307	−0.743	−0.722	−0.021
120324	−0.796	−0.722	−0.074
120991	−0.873	−0.722	−0.151
124367	−0.592	−0.522	−0.070
127972	−0.701	−0.754	0.053
131492	−0.769	−0.522	−0.247
137387	−0.688	−0.785	0.097
142983	−0.170	−0.456	0.286
148184	−0.938	−0.754	−0.184
155806	−0.977	−0.908	−0.069
157042	−0.766	−0.722	−0.044
158427	−0.613	−0.722	0.091
167128	−0.631	−0.589	−0.042
173948	−0.780	−0.722	−0.058
178175	−0.630	−0.722	0.092
205637	−0.516	−0.656	0.140
209409	−0.322	−0.323	0.001
212571	−1.024	−0.785	−0.239

III. BALMER LINE PHOTOMETRY

It is well known that some physical properties of the early-type stars can be derived from the H_β line. One very important parameter is the absolute magnitude, but for the Be stars this is not easy if we are employing the common procedure of measuring the H_β line (Crawford *et al.* 1975).

To resolve this problem, in addition to the H_β line, the H_α and H_γ lines were measured with the same method outlined by Crawford (1958).

The original photoelectric measures for those lines carried out in 1970 and 1972 were already presented (Feinstein 1974). Later on, more measures were obtained at different observatories: Cerro Tololo, La Silla (both in Chile), and Porto Alegre (Brazil). Also additional

TABLE III. Percentage of variability.

	Ferrer and Jaschek (1971)		This work	
	Limit[a]	% variable	Limit[b]	% variable
V	$0^{m}_{.}04$	53	$0^{m}_{.}025$	77
$B-V$	0.022	56	0.015	48
$U-B$	0.04	35	0.020	68

[a] All stars with dispersions larger than this limit are considered variables.
[b] Values used as upper limits for the matchings between the B and Be dispersion distributions.

measures in H_β made in 1968, but not presented before, are included here.

As usual, the instrumental system of the β index was transformed into the standard system through the list of standard stars given by Crawford and Mander (1966), plus a few more stars in the southern hemisphere from the list of Crawford, Barnes, and Golson (1970). The α and γ indices for the standard stars were taken from Table II of Feinstein (1974).

The filters for the H_α and H_γ lines employed at Cerro Tololo were always those which defined the system (Feinstein 1974), but for the H_α measures at Porto Alegre, a set of interference filters made by Infrared Industries was used. A good agreement from the comparison of the measures suggests that there are no systematic effects in the transformation.

The average values of the indices for the Be standard stars, the dispersion in each index and the number of measures are presented in Table IV. The mean-square

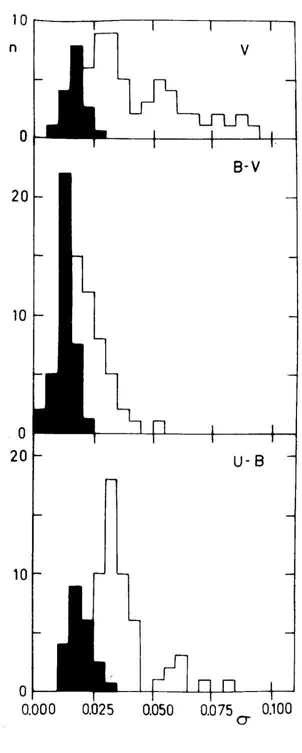

FIG. 4. The distribution of the observed dispersions of the V, $B-V$, and $U-B$ for the Be stars. The dark area is the inferred distribution of the fraction considered nonvariable.

errors for the indices measured at different observatories and for stars not extrapolated in the reductions, are about $\epsilon_{PA} = \pm 0.012$ (Porto Alegre), $\epsilon_{CT} = \pm 0.007$ (Cerro Tololo), and $\epsilon_{LS} = \pm 0.005$ (La Silla).

The β vs α diagram for all measured Be stars is plotted in Fig. 5, where the sequence for the normal stars obtained by Feinstein (1976) is also presented.

The Be stars may have changes in the emission of the Balmer lines. In this case the variations displayed by the α and β indices appear in two different ways. Some of the Be stars show differences between the average of our measures and those reported in the literature (see i.e., Lindemann and Hauck 1973). Another possibility of detecting the amount of variation in the indices is through the analysis of the frequency histograms of the dispersions.

But, before doing this, we have to look for possible causes of errors in these quantities. Because of the particular location of Be stars in the β vs α diagram relative to normal stars (see Fig. 5), and as standard stars are selected only amongst the normal stars, we have the unfortunate situation that, in the photometric reduction of each observing night, the solution obtained with the standard stars must be extrapolated to give the indices of most emission-line stars. This situation is five times worse in the α index than in the β index. To look for errors introduced by this circumstance, we have plotted the observed dispersion in each index versus the proper index in Figs. 6 and 7. A dashed line was also drawn to distinguish the stars extrapolated in the solution $\alpha < 1^{m}_{.}44$ and $\beta < 2.53$, from those that are not. The foreseen effect is clearly present in the α index dispersions but no effect appears in β. Therefore the σ_α should be used with extreme care for statistical purposes as it is clearly contaminated by extrapolation errors.

Figure 8 shows the distribution of the observed dispersions in the α, β, and γ indices of the Be stars, as well as those of a suitable number of non-emission comparison stars observed simultaneously with the former. Leaving aside the σ_α, the distribution of the emission and non-emission dispersions are similar, and we find that about 15% of the Be stars have β indices indicating variability, the fraction being smaller for the γ index.

This result is obtained over a 4- to 8-year interval of measurements that is shorter than the 13 year interval quoted by Feinstein (1973), which gives a larger percentage of variations. This fact indicates that the $H\beta$ line variations are mostly of long-term character.

The stars with dispersions $\sigma_\alpha > 0^{m}_{.}04$ and $\sigma_\beta > 0^{m}_{.}03$ are listed in Table V, with an indication of some other data which presumably may denote peculiarities. We notice that in many cases such stars are characterized by small α indices ($\alpha < 1^{m}_{.}40$), but also large σ_V which suggests that in all of them the changes are displayed in the $H\alpha$ emission as well as in the magnitude.

TABLE IV. Observed α, β, and γ indices of the Be stars.

HD	α	β	γ	σ_α	σ_β	σ_γ	n	n	n
28497	1.320	2.464	2.044	0.017	0.016	0.008	11	12	11
30076	1.302	2.470	2.058	0.027	0.024	0.008	11	18	11
35165	1.452	2.597	2.114	0.026	0.014	0.007	8	11	8
37795	1.420	2.643	2.171	0.016	0.009	0.004	7	16	7
41335	1.294	2.456	2.054	0.048	0.015	0.022	9	8	9
42054	1.408	2.605	2.153	0.015	0.035	0.005	6	7	6
43544	1.436	2.579	2.131	0.034	0.016	0.038	7	7	7
44458	1.292	2.453	2.035	0.063	0.007	0.013	6	6	6
45677	0.992	2.305	2.021	0.070	0.048	0.027	10	10	8
45910	1.290	2.440	2.059	0.076	0.029	0.020	9	9	9
48917	1.384	2.519	2.051	0.020	0.025	0.004	5	5	5
50013	1.361	2.478	2.043	0.011	0.013	0.005	4	4	4
52437	1.469	2.612	2.167	0.021	0.017	0.006	6	6	6
54309	1.291	2.460	2.065	0.044	0.073	0.015	6	6	6
56014	1.417	2.568	2.096	0.009	0.019	0.009	10	12	10
56139	1.345	2.522	2.083	0.027	0.020	0.018	8	9	8
57150	1.341	2.502	2.089	0.076	0.072	0.033	5	6	5
58155	1.438	2.606	2.103	0.016	0.025	0.012	5	6	5
58343	1.351	2.566	2.114	0.025	0.014	0.001	4	4	4
58978	1.357	2.494	2.044	0.032	0.011	0.008	4	4	4
60606	1.258	2.469	2.061	0.036	0.005	0.007	4	4	4
60855	1.472	2.614	2.106	0.018	0.010	0.008	5	5	5
61925	1.460	2.612	2.139	0.024	0.013	0.011	5	5	5
63462	1.368	2.479	2.030	0.025	0.011	0.008	4	4	4
65875	1.195	2.445	2.053	0.032	0.010	0.006	4	3	4
66194	1.410	2.548	2.098	0.025	0.033	0.012	3	3	3
67888	1.386	2.562	2.117	0.023	0.016	0.005	5	4	5
68980	1.282	2.405	2.017	0.035	0.031	0.005	4	5	4
72067	1.444	2.624	2.124	0.015	0.008	0.026	5	4	5
75311	1.463	2.620	2.139	0.018	0.022	0.007	6	6	6
77320	1.387	2.549	2.080	0.015	0.011	0.007	6	7	6
78764	1.428	2.552	2.078	0.015	0.016	0.021	6	6	6
83953	1.366	2.591	2.145	0.029	0.014	0.006	17	18	8
86612	1.326	2.580	2.147	0.040	0.026	0.019	9	10	9
88661	1.283	2.445	2.035	0.022	0.020	0.008	6	7	5
88825	1.364	2.578	2.129	0.027	0.005	0.006	7	8	6
89890	1.470	2.612	2.134				2	2	2
91465	1.314	2.501	2.073	0.037	0.011	0.009	6	6	5
92964	1.453	2.517	2.033	0.013	0.016	0.008	9	9	9
102776	1.452	2.636	2.160	0.013	0.015	0.007	8	8	6
105435	1.306	2.460	2.051	0.023	0.014	0.009	9	7	7
105521	1.449	2.578	2.106	0.020	0.016	0.008	9	9	7
106911	1.488	2.693	2.204	0.015	0.014	0.006	8	8	6
110432	1.264	2.372	1.990	0.023	0.010	0.006	8	8	6
112078	1.483	2.676	2.172	0.004	0.012	0.014	6	5	4
112091	1.309	2.591	2.166	0.031	0.018	0.004	8	8	6
113120	1.353	2.491	2.043	0.024	0.046	0.008	4	4	3
115842	1.426	2.510	2.047	0.009	0.041	0.005	5	5	3
120307	1.476	2.614	2.125	0.005	0.012	0.002	6	6	3
120324	1.398	2.558	2.083	0.065	0.053	0.012	5	5	3
120991	1.345	2.486	2.057	0.039	0.008	0.003	4	4	3
124367	1.245	2.532	2.124	0.028	0.007	0.007	5	5	3
127972	1.471	2.607	2.108	0.003	0.008	0.005	4	4	4
131492	1.406	2.597	2.121	0.025	0.027	0.011	5	5	4
137387	1.288	2.497	2.060				3	3	3
142983	1.340	2.565	2.131	0.035	0.005	0.003	4	4	4
148184	1.181	2.399	2.021	0.056	0.046	0.004	4	8	4
148379	1.454	2.499	2.045				3	3	3
148688	1.428	2.521	2.052	0.014	0.011	0.008	4	4	4
149404	1.418	2.514	2.004				2	2	2
152235	1.443	2.524	2.057				3	3	3
152236	1.416	2.474	2.025	0.005	0.012	0.010	4	4	4
152667	1.424	2.502	2.041				2	2	2
154090	1.433	2.534	2.060	0.001	0.013	0.005	2	4	2
155806	1.300	2.498	2.035				2	3	2
157042	1.255	2.473	2.064				1	1	1
158427	1.206	2.485	2.100				1	1	1
167128	1.419	2.582	2.104	0.019	0.012	0.004	3	9	3
173948	1.425	2.574	2.085	0.023	0.011	0.007	2	15	2
178175	1.426	2.564	2.099	0.021	0.008	0.006	2	9	2
205637	1.384	2.566	2.107	0.030	0.010	0.005	4	13	4
209014	1.410	2.678	2.201	0.014	0.005	0.015	3	11	3
209409	1.347	2.598	2.166	0.032	0.010	0.005	5	9	5
209522	1.463	2.593	2.138	0.007	0.012	0.013	4	9	4

TABLE IV. (Continued).

HD	α	β	γ	σ_α	σ_β	σ_γ	n	n	n
212571	1.302	2.413	2.025	0.039	0.031	0.008	7	14	7
214748	1.433	2.666	2.187	0.013	0.005	0.008	5	16	5

IV. THE EMISSION INDICES

We define here the emission indices e_α and e_β of the Be stars as the differences between the observed values of the indices α and β and those of a normal star with the same spectral type characteristics but without emission: α_0 and β_0. These balmer line indices for stars without emission are approximated by the expression:

$$\alpha_0 = c\beta_0 + d, \quad (1)$$

where $c = 0.2133$ and $d = 0.912$. (2)

The emission-line ratio e_β/e_α was studied by Feinstein (1976), cf Table II of that paper, and here we use the approximation

$$e_\beta/e_\alpha = (\beta_0 - \beta)/(\alpha_0 - \alpha) = b\beta_0 + a, \quad (3)$$

where $a = 9.667$ and $b = -3.333$. (4)

Therefore, the observed indices α, β of the emission-line stars can be converted in the values α_0, β_0 of the same stars after subtracting the emission line effects. The procedure consists in solving the system of equations formed by (1) and (3). Then, the β_0 value is obtained as one of the roots (using the negative value of the square root) of the second-degree equation:

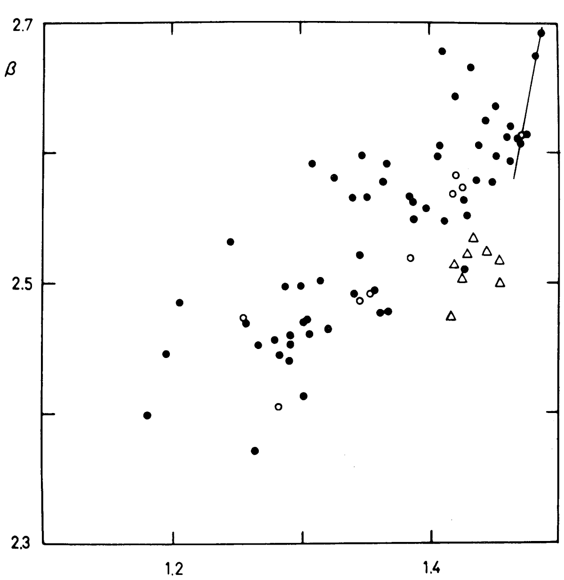

FIG. 5. The β versus α diagram for the Be stars. The line is the sequence for the normal stars taken from Feinstein (1976). The symbols are the same as in Fig. 1.

$$A\beta_0^2 + B\beta_0 + C = 0, \quad (5)$$

where
$$A = bc,$$
$$B = b(d - \alpha) + ac - 1, \quad (6)$$
$$C = a(d - \alpha) + \beta.$$

α_0 can then be obtained from Eq. (1), and the emission indices simply through

$$e_\alpha = \alpha_0 - \alpha, \quad e_\beta = \beta_0 - \beta. \quad (7)$$

The computed values of β_0, e_α, and e_β are listed in Table VI.

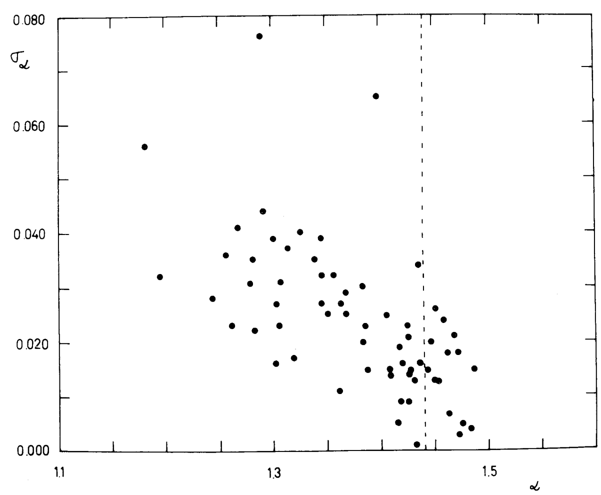

FIG. 6. The dispersion σ_α versus α for the Be stars.

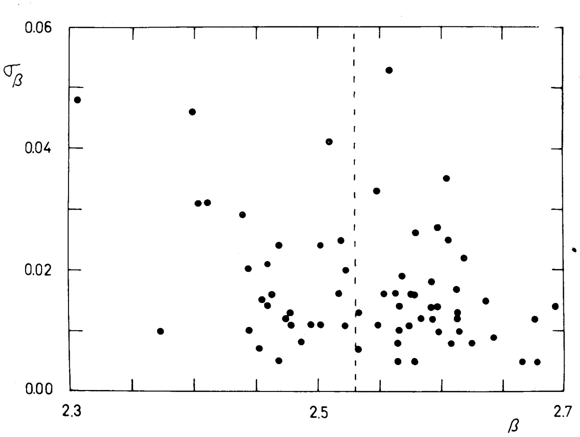

FIG. 7. The dispersion σ_β versus β for the Be stars.

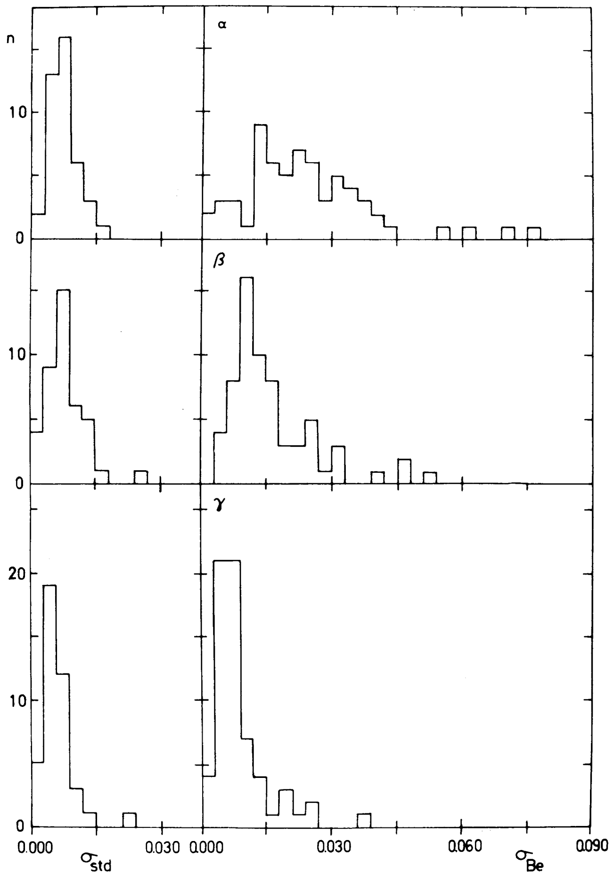

FIG. 8. The frequency distribution of the observed dispersions in α, β, and γ indices for the Be and B stars.

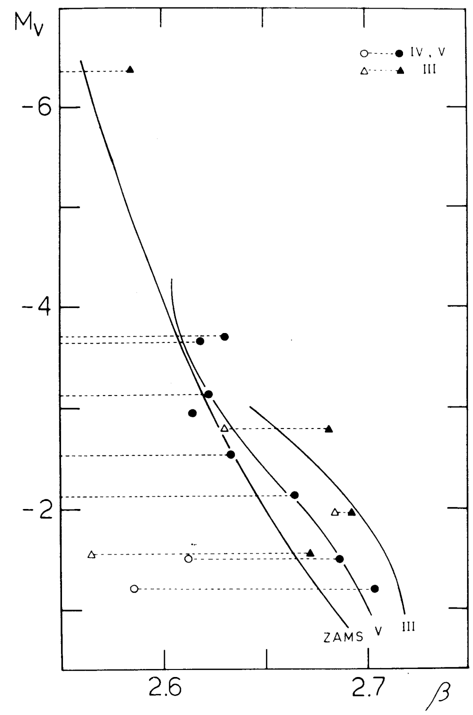

FIG. 9. The relation of M_V vs the β_0 index for the Be stars belonging to clusters and associations (see text).

We shall demonstrate here that the de-emissioned value β_0 of a Be star is an absolute magnitude indicator as good as the β value of normal stars. Twelve Be stars belonging to clusters and associations were selected because their distances are well known. For those stars the computations were made with only α and β indices measured simultaneously. In Fig. 9 their absolute magnitudes are plotted against the de-emissioned index β_0. The results are tabulated in Table VII. The observed β values were also included in the same figure and connected to the corresponding β_0 values by dashed lines. The (β, M_V) calibration of Crawford (1978), as represented in his Fig. 24, is also plotted. It is noted that stars of different luminosity are clustered along the corresponding lines.

TABLE V. Be stars with dispersions $\sigma_\alpha > 0^m.04$ or $\sigma_\beta > 0^m.03$.

HD	σ_α	σ_β	α	σ_V
42054	0.015	0.035	1.408	0.028
44458	0.041	0.007	1.269	0.041
45677	0.070	0.048	0.992	0.161
45910	0.076	0.029	1.290	0.039
54309	0.044	0.021	1.291	0.055
66194	0.025	0.033	1.410	0.034
68980	0.035	0.031	1.282	0.106
86612	0.040	0.026	1.326	0.076
115842	0.009	0.041	1.426	0.022
120324	0.065	0.053	1.398	0.123
148184	0.056	0.046	1.181	0.079
212571	0.039	0.031	1.302	...

Turning now again to the emission indices e_α and e_β, we have compared them with the corresponding values obtained through the visual inspection of spectrograms by Lesh (1968), and by Hiltner, Garrison, and Schild (1969). This system ranges from no indication of emission to the strongest emission features indicated by the symbols 1, 1+, 2, 2+, 3, 3+, and 4, subindexed to the letter e at the end of the MK spectral type designation. The Balmer lines observed for emission are those confined to the blue, and of course the Hα line is not included.

Figure 10 shows the comparison of both systems for only those stars which have 4 or more photometric measures. Part a shows the comparison with the e_α index, while part b with the e_β index. Assigning the values 1.5, 2.5, and so on to the symbols 1+, 2+, . . . , the regression lines of the spectroscopic emission index (em) against the photometric indices were computed. For 47 stars the results become:

$$\text{em} = 12.72\, e_\alpha - 0.03, \quad r = 0.81, \quad \sigma_{\text{em}} = 0.69, \quad (8)$$

$$\text{em} = 15.52\, e_\beta - 0.07, \quad r = 0.86, \quad \sigma_{\text{em}} = 0.60, \quad (9)$$

where r is the correlation coefficient and σ_{em} the dis-

TABLE VI. The corrected β_0 index and the emission indices e_α and e_β.

HD	β_0	e_α	e_β
28497	2.609	0.148	0.145
30076	2.626	0.170	0.156
35165	2.614	0.018	0.017
37795	2.690	0.066	0.047
41335	2.630	0.193	0.174
42054	2.662	0.072	0.057
43544	2.611	0.033	0.032
44458	2.635	0.205	0.182
45677	2.674	0.490	0.369
45910	2.612	0.179	0.172
48917	2.602	0.083	0.083
50013	2.586	0.103	0.108
52437	2.613	0.000	0.001
54309	2.648	0.186	0.156
56014	2.619	0.054	0.051
56139	2.636	0.129	0.114
57150	2.627	0.169	0.155
58155	2.639	0.037	0.033
58343	2.667	0.130	0.101
58978	2.604	0.110	0.110
60606	2.651	0.220	0.182
60855	2.612	0.003	0.002
61925	2.623	0.012	0.011
63462	2.580	0.094	0.101
65875	2.667	0.286	0.222
66194	2.605	0.058	0.057
67888	2.640	0.089	0.078
68980	2.593	0.183	0.188
72067	2.652	0.034	0.028
75311	2.629	0.010	0.009
77320	2.627	0.085	0.078
78764	2.590	0.037	0.038
83953	2.678	0.117	0.087
86612	2.692	0.160	0.112
88661	2.621	0.188	0.176
88825	2.669	0.117	0.091
89890	2.612	−0.001	0.000
91465	2.641	0.161	0.140
92964	2.510	−0.005	−0.007
102776	2.658	0.027	0.022
105435	2.616	0.164	0.156
105521	2.595	0.017	0.017
106911	2.692	−0.002	−0.001
110432	2.583	0.199	0.211
112078	2.676	0.000	0.000
112091	2.707	0.181	0.116
113120	2.614	0.129	0.123
115842	2.545	0.029	0.035
120307	2.607	−0.008	−0.007
120324	2.626	0.074	0.068
120991	2.607	0.123	0.121
124367	2.697	0.242	0.165
127972	2.604	−0.004	−0.003
131492	2.657	0.073	0.060
137387	2.654	0.190	0.157
142983	2.673	0.142	0.108
148184	2.648	0.296	0.249
148379	2.482	−0.013	−0.017
148688	2.555	0.029	0.034
149404	2.560	0.040	0.046
152235	2.537	0.010	0.013
152236	2.516	0.033	0.042
152667	2.538	0.029	0.036
154090	2.563	0.026	0.029
155806	2.647	0.177	0.149
157042	2.656	0.223	0.183
158427	2.685	0.279	0.200
167128	2.631	0.054	0.049
173948	2.617	0.045	0.043
178175	2.606	0.042	0.042
205637	2.645	0.092	0.079
209014	2.727	0.084	0.049
209409	2.694	0.140	0.096
209522	2.596	0.003	0.003
212571	2.583	0.161	0.170
214748	2.703	0.056	0.037

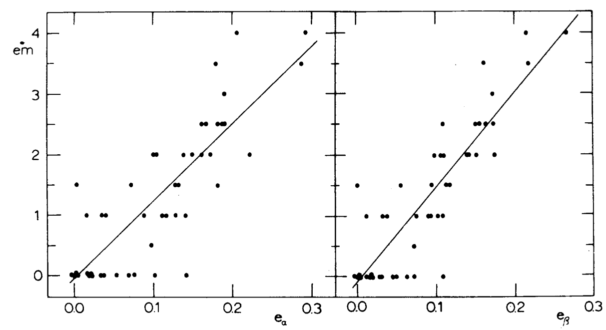

FIG. 10. The emission from visual inspection of spectrograms (em) vs the photoelectric emission indices e_α and e_β.

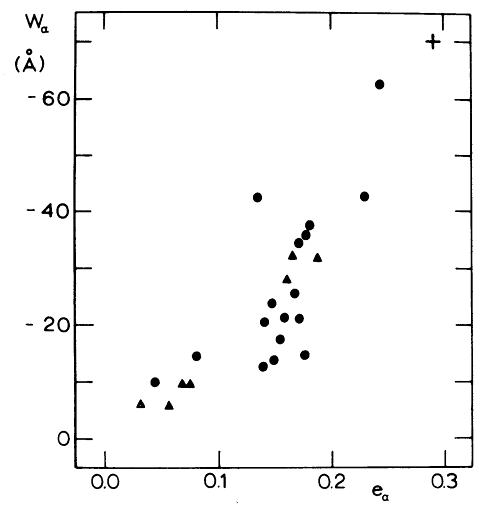

FIG. 11. The emission index e_α versus the equivalent width Wα. Circles are used for photographic determinations of $W\alpha$, triangles for photoelectric. The plus sign corresponds to χ Oph determined photoelectrically by Gray and Marlborough (1974).

persion of the spectroscopic emission indices relative to the regression line. As expected, the best correlation is obtained with the e_β index, since the spectroscopic observations are confined to the blue.

Finally, the emission indices e_α and e_β are compared in Figs. 11 and 12 with the emission equivalent width $W\alpha$ and $W\beta$, respectively. The equivalent widths were obtained from the works of Briot (1971), Bahng (1976), and Dachs *et al.* (1977). The shape of the observed

TABLE VII. Data for Be stars in clusters and associations.

HD	cluster	$V - M_v$	M_v	β	β_0	Sp. T.
22192	α Per	6.35	−2.12	2.483	2.665	B2/Ve$_2$
23302	Pleiades	5.65	−1.95	2.684	2.693	B6/III
23480	Pleiades	5.65	−1.49	2.613	2.687	B6/IV
23630	Pleiades	5.65	−2.78	2.631	2.682	B7/III
60855	NGC 2422	8.65	−2.95	2.615	2.615	B2/Ve$_{1+}$
66194	NGC 2516	8.36	−2.54	2.547	2.634	B2/IVpne$_{1+}$
105435	Sco-Cen	6.17	−3.65	2.463	2.619	B2/IVne$_{2+}$
110432	NGC 4609	11.68	−6.38	2.371	2.585	B2/?pe$_4$
112091	Sco-Cen	6.30	−1.20	2.586	2.704	B5/Vne$_{1+}$
120324	Sco-Cen	7.16	−3.69	2.515	2.631	B2/IV-Ve$_3$
142983	Sco-Cen	6.34	−1.54	2.565	2.673	B5/IIIp
148184	Sco-Cen	7.52	−3.13	2.355	2.623	B1.5/Ve$_4$

relation can be understood if we remember certain features: (a) In contrast to the case for the spectroscopic emission index whose comparison we have just presented, the observations were not obtained simultaneously. (b) The equivalent width corresponding to $e_\alpha = e_\beta = 0$ is not constant but varies with spectral type. As a consequence, we are expecting a kind of band rather than a narrow regression line. (c) When the emission line is weak, the observer carefully assumes the shape of the underlying absorption line and gives the equivalent width of the *emission feature only.* As the emission gets stronger the absorption line is filled in and finally it disappears completely; no correction is then applied. We notice in Figs. 11 and 12 that the transition between weak and strong emission lines occurs at about $e_\alpha = 0^{m}.12$ and $e_\beta = 0^{m}.10$. This situation breaks the relation into two different sections and automatically forces the weak line portion to pass through the origin.

Figure 13 is a plot of the ultraviolet excess, as measured by ΔQ, and the emission in the Balmer lines represented by the e_α index. We must remember here that observational errors, which usually are believed to be ±1 subclass for the spectral type determination (Jaschek and Jaschek 1973), lead to a dispersion of ±0.07 in the ΔQ. In spite of having used always the spectral types from the same authors for the sake of consistency, there are some obvious cases of possible errors in the classifications. The two most extreme cases of deviation we have detected from the relation e_α vs ΔQ: HD 131492 and 137387, were examined. We have searched for other spectral type classifications for both stars using the MK Catalogues of Jaschek *et al.* (1964), Kennedy and Buscombe (1974), and Buscombe (1977), and also the Michigan Spectral Catalogue (Houck and Cowley 1975). From these spectral types we conclude that the most likely classification for HD 131492 is one subclass earlier, and for HD 137387 two subclasses later than those assigned in Table I. Using the revised data we have plotted the corrected positions for these two stars together with the original ones in Fig. 13. The new positions (open circles) are in much better agreement with the general trend of the remaining points

It is clear that a correlation exists between both sets of data in the sense that the ultraviolet excess (Balmer continuum emission) is produced by the same mechanism as Balmer line emission: the gaseous envelope. A few positive ΔQ values give an indication that some stars have the Balmer discontinuity in absorption by an amount larger than predicted by the spectral type (i.e., "shell" stars), while we have no analogous situation in the lines. This fact can be explained if we recall that "shell" absorption lines are too narrow to be detected by the line measuring technique used here.

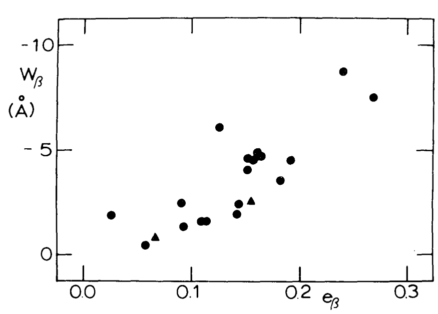

FIG. 12. The emission index e_β versus the equivalent width $W\beta$. The symbols are the same as in Fig. 12.

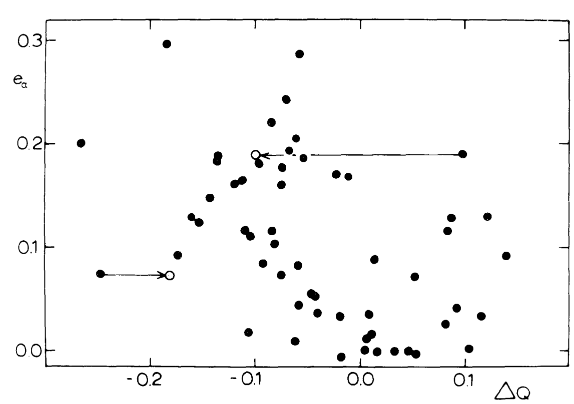

FIG. 13. The emission index e_α versus the ultraviolet excess ΔQ (see text).

V. THE ROTATIONAL VELOCITY V SIN i

Using the $V \sin i$ data from Uesugi's (1978) compilation we have represented in Fig. 14 a plot of the observed dispersion in visual magnitude, σ_V, versus the projected rotational velocity. Within the frame of the presently accepted model for Be stars, the observed decrease of overall brightness variations for the stars of high-projected rotational velocity can be explained in the following way. As it is assumed that Be stars rotate close to break-up velocity, which is almost the same for all masses, the value of $V \sin i$ is mainly a function of the inclination. Therefore, stars with high-projected rotational velocity are, on the average, seen from the equator. Two kinds of variations in the visible continuum can be foreseen for Be stars surrounded by ring-like equatorial gaseous envelopes: short- and long-term variations. The short-term variations are caused by inhomogenities in the gaseous ring, which are responsible for the variations in equator-on Be stars. On the other hand, long-term variations can be explained by an overall change of the scattering optical depth of the gaseous ring. This variation is almost cancelled for stars seen equator-on, as the observer "sees" the star dimmed when the ring is bright and *viceversa*. For perfect scattering and spherically symmetrical shells, the observed overall flux is independent of the shell's optical depth. For stars seen pole-on the variations in the extent and density of the gaseous ring may be detected as overall changes in the observed flux.

Our observations were on purpose spaced sparsely in time as we have in mind to detect long-term variations, therefore, it is not surprising that the observed dispersion of the brightness in the continuum is larger for those stars seen pole-on, i.e., those with $V \sin i \leq 285$ km/sec.

If the adopted model is correct the intensity variations of the emission lines such as Hβ, which is an indicator of the gaseous envelope's extent and density, should be correlated with the visual magnitude dispersion. The plot of the σ_V versus σ_β, only for stars seen pole-on ($V \sin i \leq 285$ km/sec), presented in Fig. 15 shows a good correlation between both quantities, even though both sets of observations are not simultaneous.

In Fig. 16 the strength of the Balmer line emission is plotted against the projected rotational velocity. Different causes of mass loss place the stars in different locations in the e_α versus $V \sin i$ plane. Supergiant emission-line stars, shown as open circles, fall in the small velocity-little emission lower left corner; extreme Be stars (Schild 1973) shown as triangles, are located in the low velocity-high emission upper left corner. The remaining stars depicted by filled circles fill up the rest of the plane. If we ascribe the majority of the remaining 13 circles located in the upper left quadrant to the extreme Be class, then we have that emission increases with $V \sin i$ for the other stars.

The final conclusion regarding the photometric data

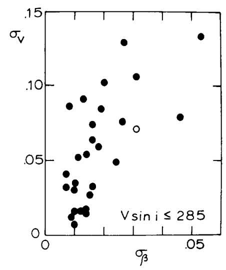

FIG. 15. The magnitude dispersion σ_V vs the β index dispersion σ_β for the Be stars with $V \sin i < 285$ km/sec. The open circle corresponds to π Aqr (Nordh and Olofsson 1977).

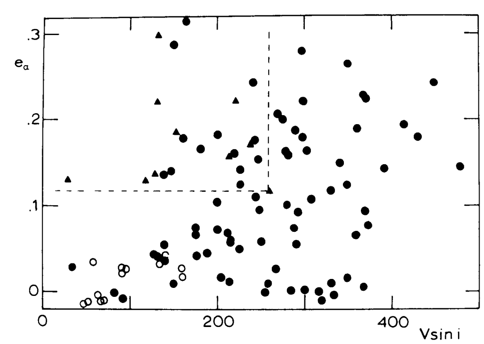

FIG. 16. The emission index e_α versus the projected rotational velocity $V \sin i$ for the Be stars. The open circles correspond to supergiant stars, the triangles are extreme Be stars according to the classification of Schild (1973), and the full circles are dwarf Be stars.

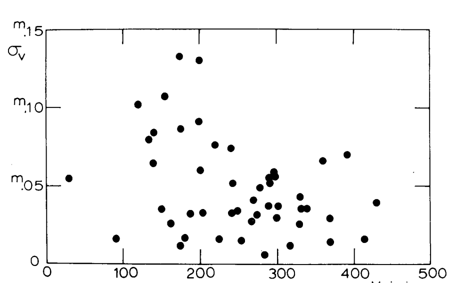

FIG. 14. The visual magnitude dispersion σ_V vs $V \sin i$.

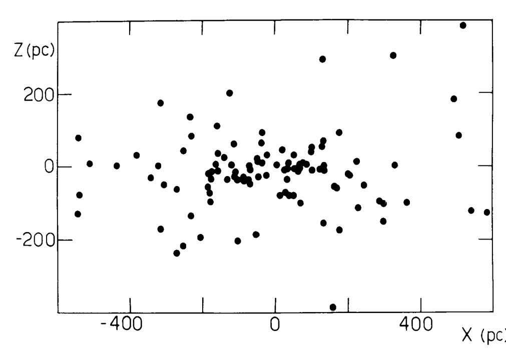

FIG. 17. The Be stars projected in a plane perpendicular to the galactic plane and in the direction center-anticenter.

and $V \sin i$ suggests that the structure of the material outside the star is distributed in a ring. When its density changes, the modification in brightness is evident only when the ring is not in the same plane as the observer.

VI. GALACTIC DISTRIBUTION

With the method outlined above, that is using β_0 and Crawford's (1978) calibration, the absolute magnitude and distance of each dwarf Be star was derived.

In Fig. 17 the Be stars are plotted in the $X - Z$ plane as defined by Stothers and Frogel (1974). No indication of the Gould's Belt appears in the distribution, but the number of stars is too low to draw any definite conclusion.

As all the observed stars are listed in the Bright Stars Catalogue ($V < 6.2$) and the intrinsically faintest Be stars have absolute magnitudes of about $M_V = -0.8$, we have a complete sample for all the Be stars that have distance modules smaller than $V - M_v = 7.0$. Assuming no interstellar absorption, our sample is complete to about 250 pc from the Sun. Taking into account this limit, we have performed a Z distribution statistic in a cylinder 200 pc radius to avoid incompleteness effects. The resulting galactic concentration parameter for the dwarf Be stars is $\beta = 40$ pc. This parameter is completely similar to that of early type B stars of population I from which the Be stars are recruited.

VII. CONCLUSIONS

The present study has been devoted to obtain information on the behavior of bright Be stars over a long period of time. From about 15 years of observations in the UBV and six to eight years in the Balmer lines, the resulting main conclusions are as follows.

(1) It is possible to obtain for each star the ultraviolet excess by means of the reddening free Q value, assuming that the spectral type is reliable.

(2) About 70% of the Be stars are variable in V and $U - B$. For $B - V$ the variability decreases to 50%. In a shorter time interval the H_β line shows variations in 15% of the Be stars. Most of the variations in the continuum and in the lines are of long-term character.

(3) The α and β values provide a way to detect the presence of hydrogen emission, the amount of which can be measured by the indices e_α and e_β. These indices appear to be well correlated to some spectroscopic features, such as equivalent widths. A dependence of e_α on the ultraviolet excess derived from the Q value also appears possible.

(4) For stars seen pole-on, the variations of the H_β line (σ_β) are correlated with the variations in the continuum (σ_V), which is in accord with a model of Be star having a ring-like gaseous envelope.

(5) For each Be star, the observed β index corrected for the emission index e_β is a good indicator of absolute magnitude. Thus it becomes possible to study the Be stars in the same way as non-emission B-type stars.

One of us (A.F.) wants to acknowledge the facilities and the hospitality provided by the Cerro Tololo Inter-American Observatory and the European Southern Observatory. Dr. E. R. Vieira of the Instituto de Fisica de UFRGS with the support of the CNPq (both of Brazil), was very kind in permitting observations at Porto Alegre. Helpful comments from C. Jaschek and J. C. Muzzio are gratefully appreciated. The collaboration of María C. F. de Correbo and A. L. Cabrera is acknowledged. This work was supported in part by the Comisión de Investigaciones Científicas, Provincia de Buenos Aires, Argentina.

REFERENCES

Abt, H. A., and Golson, J. C. (1966). Astrophys. J. **143,** 306.
Bahng, J. D. R. (1976). in IAU Symposium 70, *Be and Shell Stars,* edited by A. Slettebak (D. Reidel, Dordrecht), p. 41.
Briot, D. (1971). Astron. Astrophys. **11,** 57.
Burnichon, M. L., Chalonge, D., Divan, L., and Swings, J. P., (1967). J. Obs. **50,** 391.
Buscombe, W. (1977). *MK Spectral Classifications* (Northwestern University, Evanston).
Crawford, D. L. (1958). Astrophys. J. **128,** 185.
Crawford, D. L. (1978). Astron. J. **83,** 48.
Crawford, D. L., Barnes, J. V., and Golson, J. C. (1970). Astron. J. **75,** 624.
Crawford, D. L., Barnes, J. V., and Perry, C. L. (1975). Publ. Astron. Soc. Pac. **87,** 115.
Crawford, D. L., and Mander, J. (1966). Astron. J. **71,** 114.
Dachs, J., Maitzen, H. M., Moffat, A. F. J., Sherwood, W. A., and Stift, M. (1977). Astron. Astrophys. **56,** 417.
Feinstein, A. (1968). Z. Astrophys. **68,** 29.
Feinstein, A. (1973). in IAU Symposium 50, *Spectral Classification and Multicolor Photometry,* edited by C. C. Fehrenbach, and E. E. Westerlund, (D. Reidel, Dordrecht), p. 202.
Feinstein, A. (1974). Mon. Not. R. Astron. Soc. **169,** 171.
Feinstein, A. (1975). Publ. Astron. Soc. Pac. **87,** 603.
Feinstein, A. (1976). in IAU Symposium 70, *Be and Shell Stars,* edited by A. Slettebak (D. Reidel, Dordrecht, Holland), p. 249.
Ferrer, L., and Jaschek, C. (1971). Publ. Astron. Soc. Pac. **83,** 346.
FitzGerald, P. (1970). Astron. Astrophys. **4,** 234.
Gray, D. F., and Marlborough, J. M. (1974). Astrophys. J. Suppl. **27,** 121.
Gutiérrez-Moreno, A. (1975). Publ. Astron. Soc. Pac. **87,** 805.
Hiltner, W. A., Garrison, R. F., and Schild, R. E. (1969). Astrophys. J. **157,** 313.
Houck, N., and Cowley, A. P. (1975). *Michigan Spectral Catalogue* (University of Michigan, Ann Arbor).

Jaschek, C., Conde, H., and Sierra, A. C. (1964). *Catalogue of Stellar Spectra Classified in the Morgan-Keenan System* (La Plata University, La Plata).

Jaschek, C., and Jaschek, M. (1973). in IAU Symposium 50, *Spectral Classification and Multicolor Photometry,* edited by C. C. Fehrenbach, and B. E. Westerlund (D. Reidel, Dordrecht), p. 43.

Jaschek, C., Jaschek, M., and Kucewicz, B. (1964). Z. Astrophys. **59,** 108.

Kennedy, P. M., and Buscombe, W. (1974). *MK Spectral Classifications* (Northwestern University, Evanston).

Lesh, J. R. (1968). Astrophys. J. Suppl. **17,** 371.

Lindemann, E., and Hauck, B. (1973). Astron. Astrophys. Suppl. **11,** 119.

Nordh, H. L., and Olofsson, S. G. (1977). Astron. Astrophys. **56,** 117.

Polidan, R. S., and Peters, G. J. (1976). IAU Symposium **70,** *Be and Shell Stars,* edited by A. Slettebak (D. Reidel, Dordrecht), p. 59.

Schild, R. (1973). Astrophys. J. **179,** 221.

Stothers, R., and Frogel, J. A. (1974). Astron. J. **79,** 456.

Uesugi, A. (1978). Preprint.